J Therm Spray Tech
https://doi.org/10.1007/s11666-021-01176-0

PEER REVIEWED

Monte Carlo Simulation of the Cold Spray Process of Mixtures of Metal and Ceramic Powders

S. V. Klinkov[1] · V. F. Kosarev[1]

Submitted: 23 July 2020 / in revised form: 19 January 2021 / Accepted: 31 January 2021

Abstract During cold spraying of ceramic and metal mixtures, there is an interaction between the ceramic and metal particles during the spray process; as a result, under certain conditions, a non-monotonic dependence of deposition efficiency on the content of ceramic particles in the initial powder mixture is observed. In the present work, a numerical Monte Carlo model is put forward for the first time to simulate such behavior of deposition efficiency. The calculation results were compared with the available experimental data. It is shown that, with a proper choice of the values of involved model parameters, one can invent an adequate quantitative description of both the behavior of the deposition efficiency of the mixture and the behavior of the ceramic content of the coating. Additionally, the effects of particle size, particle size distribution, and deposition efficiency of pure metal powder are discussed.

Keywords ceramic content in coating · cermets · cold spray · deposition efficiency · metal-ceramic composite · Monte Carlo simulation

List of Symbols

c_V	Volumetric content of ceramic particles in powder
c_{Vc}	Volumetric content of ceramics in coatin
c_M	Mass (weight) content of ceramic particles in powder
d_p	Size of metal particles
d_{cer}	Size of ceramic particles
DE_{mix}	Deposition efficiency of powder mixture
p	Probability of adherence of metal particles to non-activated surfaces, i.e., deposition efficiency of pure metal powder (without ceramic admixture)
p_a	Probability of adherence of metal particles to activated surfaces
p_{cer}	Probability of adherence of ceramic particles to metal surfaces
s_{a1}	Fraction of activated surface within the contact spot of a random metal particle with the coating surface
s_{cer1}	Fraction of ceramic surface within the contact spot of a random ceramic particle with the coating surface
ϑ	Probability of adherence of a random metal particle to the coating surface
ϑ_{cer}	Probability of adherence of a random ceramic particle to the coating surface

Introduction

Cermet composites are recognized as promising materials that successfully combine the ductility of metals and, simultaneously, the hardness and wear resistance of ceramics. The most widely known method for the synthesis of such composites is the compaction (pressing) of a mixture of different powders, followed by its sintering. An alternative method for the synthesis of cermet composites is the gas spraying of powder materials and, in particular,

✉ V. F. Kosarev
vkos@itam.nsc.ru

S. V. Klinkov
klyiii@yandex.ru

[1] Khristianovich Institute of Theoretical and Applied Mechanics, Siberian Branch of Russian Academy of Sciences (ITAM SB RAS), Institutskaya 4/1, Novosibirsk, Russia 630090

Published online: 22 March 2021

cold spraying. The essence of a cold spray process consists in the acceleration of powder-mixture particles to sufficiently high speeds, which allow the formation of a dense composite coating from those particles upon their impacts onto the substrate surface. The deposition process proceeds at temperatures much lower than the melting point of the mixture components; this circumstance provides for non-occurrence of phase transformations and chemical reactions between the components. If necessary, the product obtained can be given a further heat treatment.

The cold spray method was first developed at the Institute of Theoretical and Applied Mechanics (ITAM), Siberian Branch of the Russian Academy of Sciences, after the phenomenon of coating formation from non-melted metal particles was discovered in experiments on studying two-phase (gas plus metal particles) wind-tunnel supersonic flows past bodies (Ref 1,2). The deposition of coatings from mixtures of metal and ceramic powders by the cold spray method was first proposed at the Obninsk Center for Powder Spraying (Ref 3). Presently, much research on this matter is under way (see, e.g., publications; Ref 4-33). The importance of such studies is related with the possibility of production of cold-sprayed coatings with unique properties. For example, an introduction of a ceramic component into a coating can substantially increase the coating microhardness (Ref 6-9,12,15,16,21-23) and adhesion (Ref 6-9,14,15,21,22), improve the frictional properties and reduce the wear (Ref 8,12,16,21,22,27), allow fabricating coatings with a good protection against neutrons (Ref 23-26), etc.

It should be noted here that, unlike metal particles, ceramic particles almost never undergo plastic deformation upon impact, and their attachment to the coating surface is ensured due to their embedment into the metal surface layer (as occurs when a rigid body impinges onto a ductile substrate). As the metal particles present in the mixture stick to the coating surface, the coating thickness gradually increases, and the previously deposited ceramic particles get "sunk" into the metal coating formed. In the absence of metal particles, subsequent impacts of ceramic particles lead to the removal of the previously deposited particles from the surface; the latter process almost always leads to substrate–surface erosion (Ref 34, 35).

An important feature of the cold spraying of mixtures is the interaction between the metal and ceramic particles during the spray process; as a result, under certain conditions, a non-monotonic dependence of deposition efficiency on the concentration of ceramic particles in the initial powder mixture is observed (Ref 5-17,21). On increasing this concentration, the deposition efficiency of the mixture first increases, then reaches a maximum, and, afterwards, it again decreases to zero or even down to some negative value (at 100% content of ceramic particles in the spray stream with no metal particles contained in it). When the content of ceramic particles in the sprayed mixture is zero (i.e., when only metallic particles are present in the stream), the deposition efficiency is usually not equal to zero. Its magnitude depends on the spraying conditions (temperature, pressure, type of gas, particle size and shape, etc.) and on the particle and substrate materials used. Presently, no adequate theory that would allow one to reliably predict the value of deposition efficiency available; that is why this quantity, being an important characteristic of the process, is measured in experiments.

To explain the non-monotonic behavior of the deposition efficiency of cermet mixtures, a hypothesis assuming the existence of some fraction of activated area on the surface of the growing coating has been put forward. That activated area arises due to the impacts of ceramic particles, and it contributes to the adherence of metal particles to the coating surface, with a higher adherence probability in comparison with the non-activated part of the surface (that is, part of the surface that had never been hit by the ceramic particles) (Ref 5-7, 13, 21). It has been assumed (see, e.g., Ref 21) that the impacts of ceramic particles produced a specific surface roughness on the metal coating and cleaned the surface from oxide films, thereby contributing to the realization of a higher probability of metal particle adherence to the surface.

A physical and mathematical model taking into account such a two-probability nature of the interaction between the metal and ceramic particles was proposed for the first time in (Ref 13) and, via a proper choice of the values of involved empirical coefficients, it was shown that, with that model, the analyzed experimental data could be given an adequate description. In (Ref 13), the problem was solved analytically under a simplifying assumption that the ceramic particles never adhered to the coating. It should also be noted that the analytical formula for calculating the fraction due to the activated coating area within the framework of the proposed model was derived assuming that the entire activated area could be represented as a continuous surface (equal to the sum of its component parts). This approximation, being qualitatively adequate, could, however, yield quantitatively incorrect results. In practice, ceramic particles normally become incorporated in the coating, forming a fraction of the coating surface occupied by ceramic particles, and this in turn will also affect the adhesion of metal particles to the surface. In the present work, a numerical Monte Carlo model is put forward for the first time to allow both for the effect due to the adherence of ceramic particles to the coating and for the effect due to the discontinuity of both the activated surface and the surface occupied by ceramic particles.

Description of the Model

Key Points

The main initial, or input, parameters of the problem/model are: (1) the sizes of the metal d_p and ceramic d_{cer} particles, (2) the volumetric concentration c_V of ceramic particles in the powder mixture (hereinafter referred to as the ceramic content of the mixture), (3) the probabilities of adherence of metal particles to the non-activated p and activated p_a surfaces, and the probability of adherence of ceramic particles to the metal surface p_{cer}. The output parameters are the deposition efficiency of the mixture DE_{mix} (defined as the ratio between the coating mass and the powder mass spent for production of this coating) and the volumetric ceramic content of the coating c_{Vc}.

The numerical modeling consists in the following. The Monte Carlo simulation is used to determine: (1) the coordinate of the center of the particle as this particle impinges onto the surface, (2) the particle material (metal or ceramic, in accordance with the ceramic content of the mixture), and (3) the particle size complying with the particle size distribution function. If the particle turns out to be a metal particle, then the possibility of particle adherence to the surface is to be analyzed. This probability is calculated by the formula

$$\vartheta = p_a s_{a1} + p(1 - s_{a1}), \qquad \text{(Eq 1)}$$

where s_{a1} is the fraction due to the activated surface area within the contact spot of the metal particle with the coating surface. It should be noted here that both the coating surface and the contact spot of the metal particle with the coating surface are assumed to be flat, i.e., their in-plan projection is considered. In reality, the coating is rough, or three-dimensional, and the particles themselves present no flat "circles". This imposes some limitations on the applicability of the "flat" model. Some of those limitations will be considered below.

For simplicity, we further assume that the metal particles adhere to the non-activated metal surface of the coating and to the ceramic surface with identical probabilities. In other words, the coating surface formed by ceramic particles is inactive. It should be noted here that, generally speaking, these two cases (i.e., the impact of a metal particle onto the non-activated metal surface and its impact onto the ceramic surface) may differ in terms of the adherence probabilities; however, this difference is neglected here. A good agreement between the simulated and experimental data (see below) shows that this assumption is justified.

If the metal particle adheres to the coating surface, then the coating surface area equal to the area of the contact spot is assigned the status of non-activated surface.

It can be hypothesized that the rebound of a metal particle from the coating surface also leads to surface activation. However, within the framework of the present model, we assume that the surface status does not alter when a metal particle bounces from the surface area of interest. This is due to the fact that, during the interaction with the obstacle of a stream seeded just with metal particles, the coating forms under the conditions of particle adherence to, and its rebound from, the surface. The measured probability of the adherence of metal particles (i.e., the deposition efficiency of pure metal powder, without a ceramic powder additive), which is used as one of the main input parameters of the model, already includes effects related with possible activation of the coating surface due to metal particle rebounds.

If the particle impinging onto the surface is a ceramic particle, then the possibility of its adherence to the surface is to be analyzed. This probability is given by the formula

$$\vartheta_{cer} = p_{cer}(1 - s_{cer1}) \qquad \text{(Eq 2)}$$

where p_{cer} is the probability of adherence of a ceramic particle to the metal surface of the coating. Making this probability equal to zero, one can simulate the coating growth without the adherence of ceramic particles. We assume that the ceramic particle does not adhere to the ceramic surface of the coating. This explains the involvement of the factor $(1 - s_{cer1})$, where s_{cer1} is the fraction of the ceramic surface of the coating within the contact area of the ceramic particle. This assumption is based on the experimentally established fact that, when a stream involving just ceramic particles interacts with a substrate, no coating forms (see below). If a ceramic particle recoils from the coating surface, then part of the metal surface of the coating within the contact spot of the particle with the coating surface is to be assigned the status of an activated surface.

Figure 1 illustrates a model coating surface consisting of: (1) areas with surface-adhered ceramic particles (black color), (2) non-activated surface areas with surface-adhered metal particles which have not yet been hit by ceramic particles (blue color), (3) activated metal surface areas hit by the bouncing ceramic particles (red color). It can be seen that the activated area consists of small regions scattered throughout the coating surface.

A few words should be given to the erosion process. Since ceramic particles are present in the mixture, then one would expect that their impacts could cause an erosion of both the substrate and the coating. However, special experiments performed in (Ref 7,13,21) showed that the erosion of both the substrate and coating due to the impacts of ceramic particles can be neglected if the size of the latter particles is small (several tens of micrometers). This erosion can be of significance provided that the ceramic

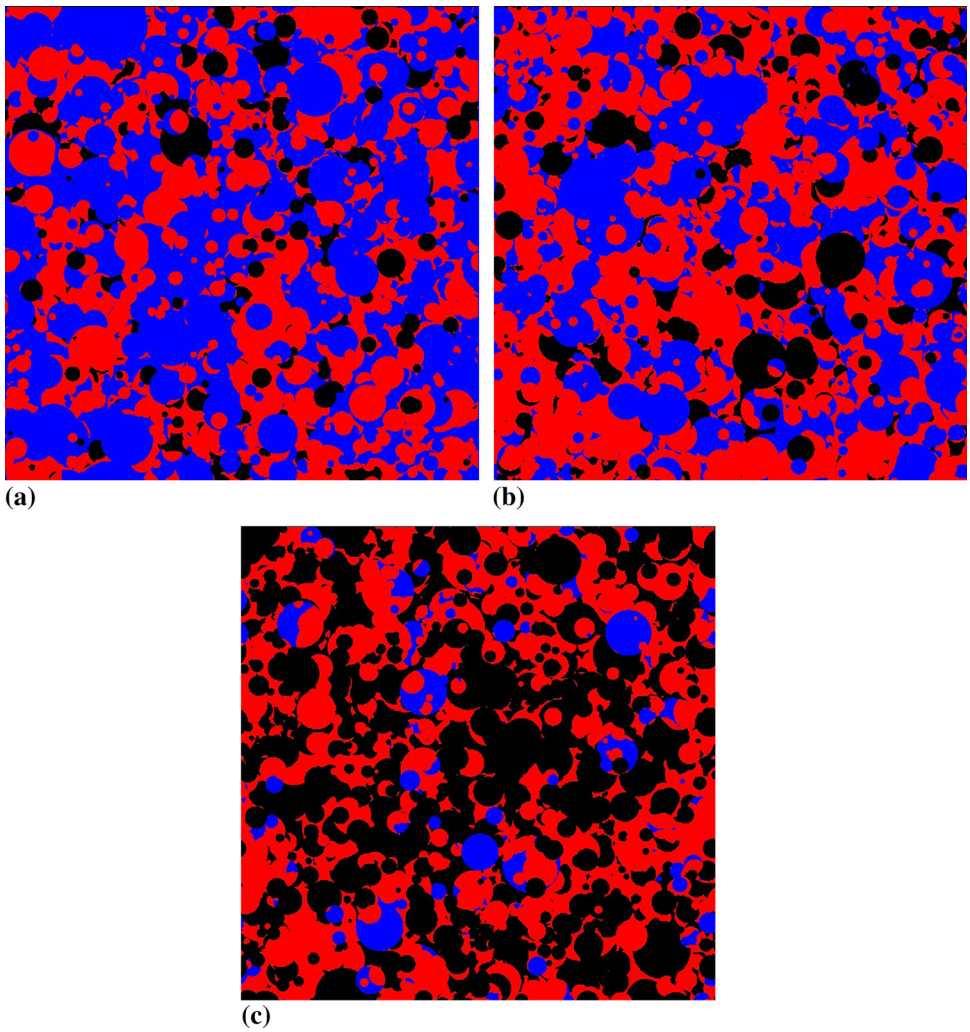

Fig. 1 The appearance of the coating surface. (a) Ceramic content of powder mixture c_V= 0.2; the fractions due to the activated and ceramic surfaces are 0.41 and 0.13, respectively; (b) c_V= 0.3, the fractions due to the activated and ceramic surfaces are 0.48 and 0.18, respectively; (c) c_V= 0.7; the fractions due to the activated and ceramic surfaces are 0.44 and 0.48, respectively

particles are relatively large (> 150 μm). Since only relatively small ceramic particles are considered below, erosion has not been taken into account in our calculations.

Particle Size Distribution Function

Volumetric size distributions of the powders were measured with aid of a size analyzer (LS 13320; Beckman Coulter, USA). For comparison of the width of these distributions, the measured distributions were normalized such a manner as to set maximum values having coordinates (1, 1). In other words, they were divided by their maximum values (which were achieved at a particle size equal to d_{pmax}) and the sizes were divided by the corresponding d_{pmax} values that are listed in the caption of Fig. 2. Corresponding maximum values (not listed in the caption) are next: 1—0.032, 2—0.075, 3—0.12, 4—0.035, 5—0.014.

The volumetric size distribution functions of the different powders in normalized coordinates $\overline{d}_{\mathrm{p}} = d_{\mathrm{p}}/d_{\mathrm{pmax}}$

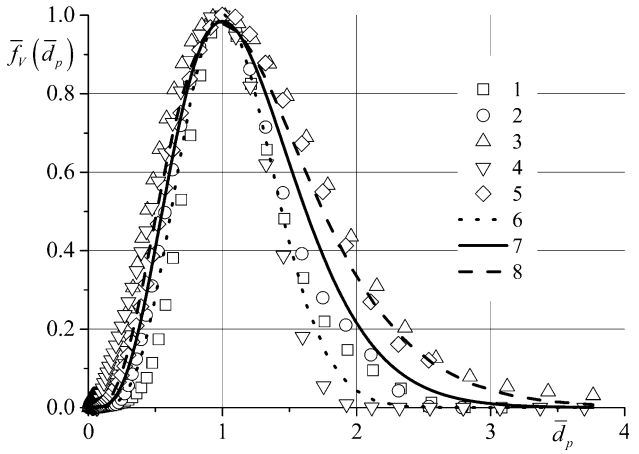

Fig. 2 Volumetric distribution of particles over particle sizes for different powders. 1–3—Silicon carbide powders: 1—d_{pmax}= 36 μm, 2—d_{pmax}= 13 μm, 3—d_{pmax}= 5.5 μm, 4—ASD-1 aluminum powder d_{pmax}= 30 μm, 5—PMS-1 copper powder d_{pmax}= 48 μm, 6–8—approximate curves calculated by Eq 3: 6—n = 2, 7—n = 1.2, 8—n = 0.9

and

$$\overline{f}_{\mathrm{V}}(\overline{d}_{\mathrm{p}}) = f_{\mathrm{V}}(d_{\mathrm{p}})/f_{\mathrm{V}}(d_{\mathrm{pmax}})$$

are shown in Fig. 2.

Also, Fig. 2 shows approximations of the distributions with an analytical equation:

$$\overline{f}_{\mathrm{V}}(\overline{d}_{\mathrm{p}}) = \overline{d}_{\mathrm{p}}^{4}\frac{\exp\left(-\frac{4}{n}\overline{d}_{\mathrm{p}}^{n}\right)}{\exp\left(-\frac{4}{n}\right)} \qquad \text{(Eq 3)}$$

Evidently, the width of the distribution can be well reproduced by Eq 3 with a properly chosen value of n.

For modeling, the approximation with n = 1.2, an average among all the other approximations, was chosen.

Choice of Calculation Domain Size

One of the problems to be solved in the present study was the necessity to choose boundary conditions so as to minimize the size of the computational domain and, hence, to reduce the time required for computation. The following boundary conditions were chosen: the upper edge was stitched with the lower edge, and the right edge with the left edge. The closed calculation domain thus formed was a torus. To verify the correctness of the choice of such boundary conditions, calculations were performed in two regions of 300 × 300 and 600 × 600 μm. Both regions were divided into meshes by a square grid with a 1-μm step. For comparison, Fig. 3 shows the deposition efficiency of the aluminum–alumina mixture and the alumina content of the coating versus the number n_{pc} of aluminum particles adhering to the surface as obtained in the calculations performed for the above-mentioned computational domains of the two different sizes (Fig. 3a and b, respectively). The calculations were performed for a mixture of aluminum and alumina particles (average particle sizes 26 and 22 μm, respectively), and for three different alumina contents of the mixture (curves 1 and 4—c_{V} = 0.1; curves 2 and 5—c_{V} = 0.4; curves 3 and 6—c_{V} = 0.7). The input parameters of the model were chosen equal to p= 0.11, p_{a}= 0.4, and p_{cer}= 0.17, which values ensured a reasonable accuracy in reproducing the results of the experiments of (Ref 21) (see below) with the model described.

It is noteworthy that, for a sufficiently large number of aluminum particles adhered to the surface, the calculations on both domains have yielded the same result. However, the calculation performed for the smaller domain led to a faster attainment of the stationary value in comparison with the calculations performed on the larger domain. Therefore, all further calculations were carried out for the smaller domain of 300 × 300 μm. The dependencies shown in Fig. 3 prove that both the stationary value of the deposition efficiency of the mixture and the stationary alumina

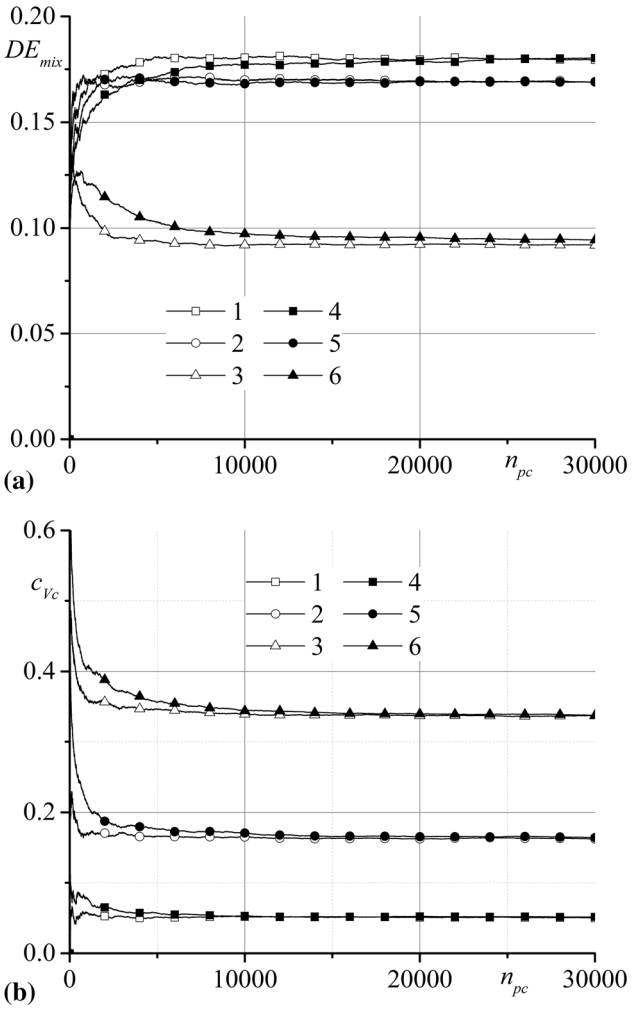

Fig. 3 The deposition efficiency of the mixture (a) and the alumina content of the coating (b) versus the number of aluminum particles adhered to the surface. The average size of the aluminum particles is d_{p}= 26 μm, and that of the alumina particles is p_{cer}= 22 μm, p= 0.11, p_{a}= 0.4, p_{cer}= 0.1. Curves 1 and 4—alumina content of the powder mixture c_{V} = 0.1; curves 2 and 5—c_{V} = 0.4; curves 3 and 6—c_{V} = 0.7, curves 1–3—calculation-domain size 300 × 300 μm, curves 4–6—calculation-domain size 600 × 600 μm

content of the coating were achieved when the total number of the aluminum particles adhered to the surface reached approximately 10,000. Later, all the performed calculations were limited to this number of adhered metal particles (10,000).

The initial substrate surface was suggested to be aluminum, i.e., made of the same material as the metal component in the powder mixture. It should be noted that, since the calculations were carried out until the stationary state, the initial substrate surface condition does not influence the results.

Verification of the Numerical Model

The model was verified according to the results of (Ref 21,22), where, unlike in other works, the most detailed experimental data on the deposition efficiency of mixtures of aluminum (d_p= 26 μm) and alumina (both irregular shape of d_{cer}= 22 μm and spherical of d_{cer}= 32 μm) powders and on the alumina content of the coating versus the alumina content of the mixture were reported. The mixtures with different alumina contents were sprayed under the same parameters: the particles were accelerated by a nitrogen flow with a stagnation pressure of 1.65 MPa and a stagnation temperature of 250 °C.

The experimental data (Fig. 6 (Ref 21,22)) and the simulated dependence of the deposition efficiency of the mixture on its alumina content are shown in Fig. 4. It should be noted that the mass concentrations used in (Ref 21,22) were recalculated into the volumetric ones using the relationship:

$$c_V = \frac{\rho_m c_M}{\rho_{cer}(1 - c_M) + \rho_m c_M}. \quad \text{(Eq 4)}$$

In this case, during the numerical simulation, the particle sizes, which were kept fixed during the calculation process, were taken to be equal to the mean experimental values (d_p= 26 μm for aluminum, d_{cer}= 22 μm for irregular alumina, and d_{cer}= 32 μm for spherical alumina). Alternatively, as the probability of adherence of aluminum particles to the non-activated surface, the experimental value obtained for the deposition efficiency of pure aluminum powder was adopted. As can be seen from Fig. 4, this probability was equal to 0.11 (Ref 21,22). Since the experimental results for mixtures with irregular and spherical alumina are different, the next two input parameters are also different. Let us first consider the results for irregular alumina. As was shown by test calculations, to match the maximum deposition efficiency obtained in the experiments (0.19 for irregular alumina; see Fig. 4a, curves 1–3), the probability of adherence of aluminum particles to the activated surface had to be taken as equal to p_a= 0.4. As an estimate of the probability of adherence of irregular alumina particles to the aluminum coating surface, we used the value p_{cer}= 0.17, which can be estimated from experimental data (see Fig. 9; Ref 21). At this value, the calculated alumina content in coating agrees well with the experimental one at low alumina content in powder (less than 0.3; see Fig. 4b, curves 1-3). The results of the calculation of the mixture deposition efficiency with the above parameters are shown in Fig. 4(a), curve 2. A fairly good agreement between the calculated and measured values is of note.

The measured (Ref 21,22) and calculated alumina contents of the coating are shown in Fig. 4(b). The calculated

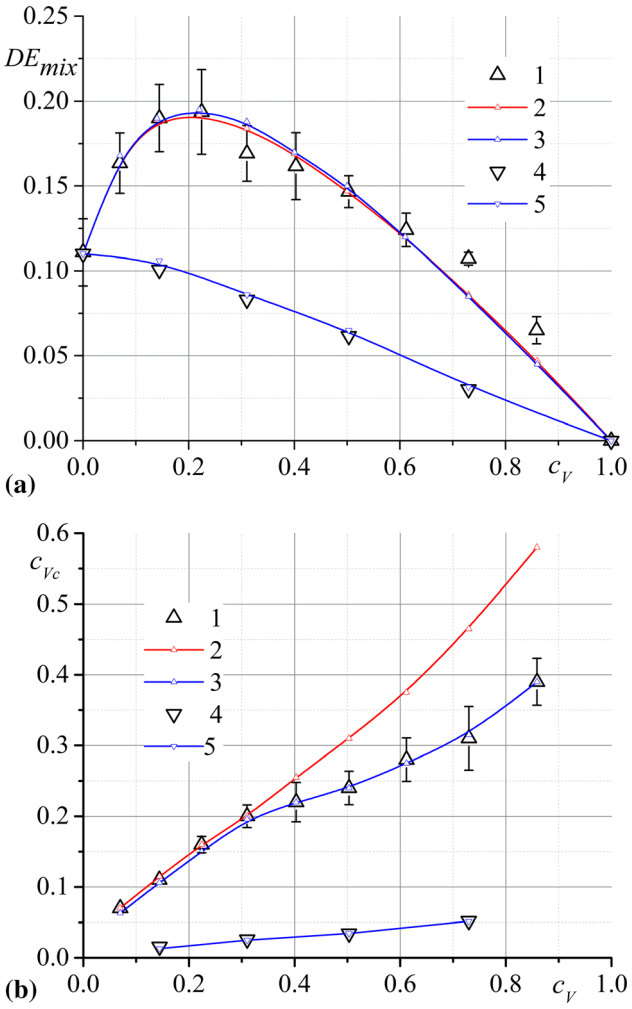

Fig. 4 Dependence of the deposition efficiency of the mixture (a) and alumina content of the coating (b) on the alumina content of the mixture. 1—Experimental results, 2—calculation with a fixed value of p_{cer} (p_{cer}= 0.17), 3——calculation with a varied value of p_{cer}. Irregular alumuna: 1—experiments, 2—calculation with a fixed value of p_{cer} (p_{cer}= 0.17), 3—calculation with a varied value of p_{cer} (Fig. 5, curve 1); spherical alumina: 4—experiments, 5—calculation with a varied value of p_{cer} (Fig. 5, curve 3)

values of this content for p_{cer}= 0.17 are shown by curve 2. It is seen that, in the latter case, the calculation yields: (1) a good agreement with the experimental data for the alumina contents of the coating being lower than 0.3, and (2) overestimated values of the alumina content of the coating at higher alumina contents of the mixture c_V.

In order to obtain agreement between the calculated and measured alumina contents of the coating, it was necessary to adjust the p_{cer} value for each value of the alumina content of the powder. Figure 5 shows the adjusted p_{cer} values. It is seen that, starting from a certain alumina content of the mixture (0.31 in Fig. 5), it is necessary to monotonically and almost linearly reduce the p_{cer} value in compliance with Eq 5.

$$p_{\text{cer}} = \begin{cases} 0.17 & \text{for } c_V \le 0.31 \\ 0.17[1 - 1.23(c_V - 0.31)] & \text{for } 0.31 \le c_V \le 1 \end{cases} \quad \text{(Eq 5)}$$

In this case, a very good agreement between the experimental and calculated data on the alumina content of the coating can be obtained (curve 3 in Fig. 4(b)).

The results of the calculation of the deposition efficiency of the mixture for this case are shown in Fig. 4(a), curve 3. It is seen that, in spite of the difference in the estimated values of p_{cer}, this parameter exerts almost no influence on the calculated deposition efficiency of the mixture.

Let us now consider the case of the mixture with spherical alumina. To fit the behavior of the mixture deposition efficiency obtained in the experiments (Fig. 4a, curves 4 and 5), the probability of the adherence of aluminum particles to the activated surface had to be taken to be equal to p_a= 0.15. As an estimate of the probability of the adherence of the spherical alumina particles to the aluminum coating surface, we adopted the linear decrease (Eq. 6) from the value p_{cer}= 0.011 (see Fig. 5, lines 3 and 4); at the adopted values, the calculated alumina content in coating agrees well with the experimental one (see Fig. 4b, curves 4 and 5).

$$p_{\text{cer}} = \begin{cases} 0.011 & \text{for } c_V \le 0.15 \\ 0.011[1 - 1.25(c_V - 0.15)] & \text{for } 0.15 \le c_V \le 1 \end{cases} \quad \text{(Eq 6)}$$

Thus, a very good agreement between the experimental and calculated data can also be obtained in the case of the powder mixture with spherical alumina.

Discussion

First, we note that the deposition efficiency of pure aluminum of 11% was obtained experimentally in (Ref 21,22), and we used this value as one of three input parameters. Second, according to Fig. 9 in (Ref 21, dark diamonds), irregular alumina deposition efficiency at low ceramic contents in the powder (10–30 wt%) is about 15%. Thus, it was *experimentally* obtained in (Ref 21) that the irregular alumina deposition efficiency at low ceramic contents is higher than the aluminum deposition efficiency. Third, p_{cer} is not a deposition efficiency of ceramic particles; according to the definition, it is a probability of the attachment of ceramic particles to metal parts of the coating surface. The ceramic deposition efficiency is defined by Eq 2. Hence, at low ceramic contents, the alumina deposition efficiency should be close to (more exactly, slightly lower than) the value p_{cer} adopted for the simulation (17%) because the coating surface consists mainly of aluminum (see, e.g., Fig. 1a), i.e., $s_{\text{cer1}} \sim 0$. For the simulation of the powder mixture with irregular alumina at a low alumina content, we adopted the value of 17%, which is close to the experimental value of 15%. For the simulation of powder mixtures with spherical alumuna at a low alumina content in the powder, the value of p_{cer} should be taken to be much lower (only 1.1%) which leads to much lower values of the alumina deposition efficiency and alumina content in the coating. At high ceramic contents, the alumina deposition efficiency should trend to zero because the coating surface consists mainly of ceramic particles (see, e.g., Fig. 1c), i.e., $s_{\text{cer1}} \sim 1$. We accept that incoming ceramic particles do not attach to ceramic particles deposited in the coating. If the metal part of the coating surface is small (i.e., the ceramic part of the coating surface is close to 1), then the attachment of ceramic particles to the coating surface is almost impossible (see Eq. 2). This lowers the ceramic deposition efficiency, but the reason why p_{cer} should be lowered is not so obvious.

The monotonic decrease in the probability of the adherence of alumina particles to the metal coating surface (p_{cer}) can be attributed to three-dimensional effects. As was noted above, in our simulations, the surface areas occupied by the ceramic and metal materials were assumed to be flat, i.e., they were the projections of these surface areas onto the plane of the coating surface that were considered. In fact, the ceramic particles become embedded in the coating, with some part of any of these particles protruding upward over the coating surface plane. This entails that the next ceramic particle, falling onto the coating near a

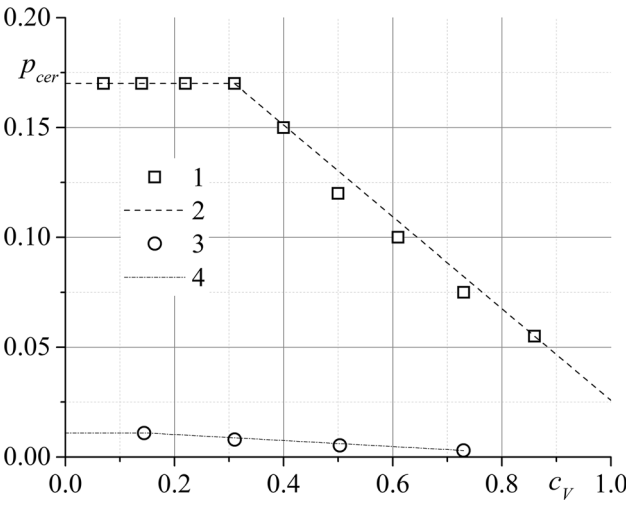

Fig. 5 Dependence of the adherence probability of alumina particles to the metal part of coating surface upon alumina content in the powder mixture. Irregular alumina: 1—adjustment according to the simulation data, 2—constant and linear approximation; spherical alumina: 3—adjustment according to the simulation data, 4—linear approximation

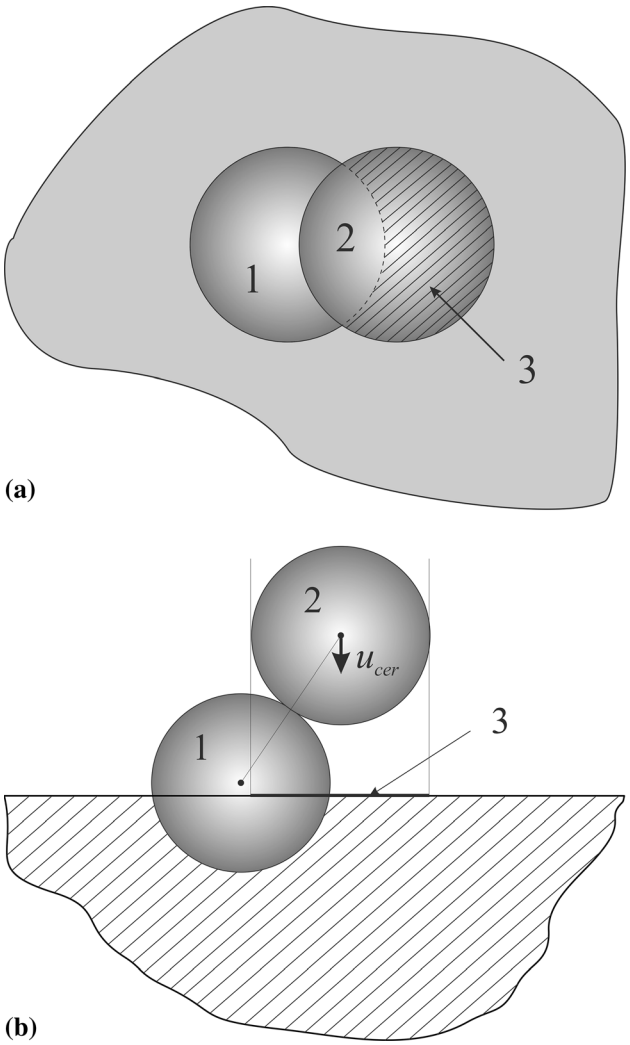

Fig. 6 An explanation of the three-dimensional effect during two ceramic particle impacts in top view (a) and side view (b). 1—First ceramic particle embedded in the coating, with some part protruding upward over the average coating surface plane, 2—the next ceramic particle, falling onto the coating near a previous one, 3—projection of the second impacting ceramic particle on the average coating surface plane

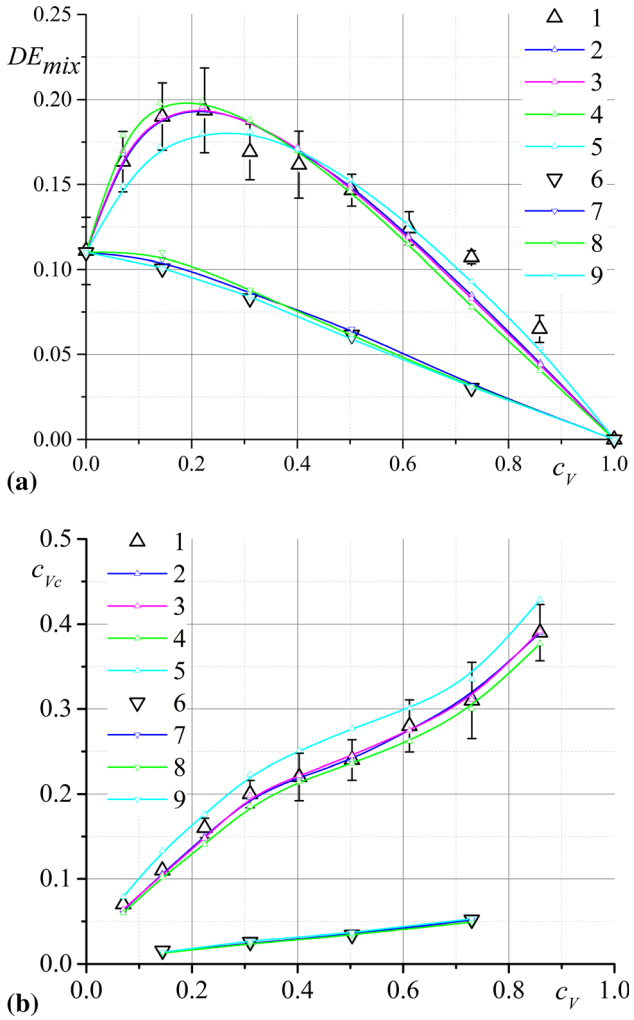

Fig. 7 The deposition efficiency of the mixture (a) and the alumina content of the coating (b) vs. the alumina content of the mixture from which the coating was sprayed. Irregular alumina: experimental results of (Ref 21,22) (curve 1), simulation of spraying with a mixture of monodispersed (curve 2) and polydispersed (curve 3) powders (d_p= 26 μm, p_{cer}= 22 μm), as well as with modified particle sizes d_p= 30 μm, p_{cer}= 20 μm (curve 4) and d_p= 20 μm, p_{cer}= 30 μm (curve 5); spherical alumina: experimental results of (Ref 21,22) (curve 6), simulation (curve 7) of spraying with a mixture of monodispersed powders (d_p= 26 μm, p_{cer}= 32 μm), as well as with modified particle sizes d_p= 30 μm, p_{cer}= 20 μm (curve 8) and d_p= 20 μm, d_{cer}= 40 μm (curve 9).

previous one, impinges onto the latter particle prior to touching the metal part of coating surface plane material (Fig. 6).

This leads to a decrease in the adherence probability of the ceramic particles. The larger the fraction of the coating surface due to the ceramic particles, the higher the probability of such an event, because, due to the lack of metal particles, the ceramic particles have no time to be sunk, partially or completely, vinside the layer of the metallic material.

In summary, we can conclude that, even within the framework of the simplified "flat" model, it is possible to adjust the main parameters of the model (p, p_a and p_{cer}) so that this model will be capable of quantitatively predicting both the behavior of the deposition efficiency of the mixture and the ceramic content of the sprayed coating with increases in the ceramic content of the powder. It is important to note that the behavior of the mixture deposition efficiency is mainly described by just two constants, namely, p andp_a. The parameter p_{cer} greatly affects the ceramic content in the coating, and it should be lowered with the increase in the ceramic content in the powder to reproduce the experimental data; this parameter does not

significantly influence the behavior of the mixture deposition efficiency.

Effect Due to the Particle Size Distribution Function

Using the above approximation of the size distribution function of the powders, we performed calculations in which the particle size was chosen at random. Data of these calculations, which were performed with all other conditions being kept identical (the same value of p_a and the same change of p_{cer}, varying from 0.17 to lower values), are shown in Fig. 7, curve 3, for the mixture with the irregular alumina. It can be seen that taking the polydispersity of the powder into account does not significantly alter the deposition efficiency of the mixture or the ceramic content of the coating sprayed from this mixture. The same very negligible difference was obtained for the case of mixtures with spherical alumina powder; for this reason, we did not show this case in Fig. 7.

Effect Due to the Particle Size

Next, we carried out calculations with different mean particle sizes. Those calculations were performed in order to examine how this size affects the results. The following two cases were analyzed. For the mixture with irregular alumina: average sizes of metal and ceramic particles d_p= 30 μm and d_{cer}= 20 μm (curve 4 in Fig. 7), and vice versa d_p= 20 μm and d_{cer}= 30 μm (curve 5 in Fig. 7). For the mixture with spherical alumina, average sizes of metal and ceramic particles d_p= 30 μm and d_{cer}= 20 μm (curve 8 in Fig. 7), and vice versa d_p= 20 μm and d_{cer}= 40 μm (curve 9 in Fig. 7). The results are shown in Fig. 6. It can be seen from Fig. 7 that, in the case of mixture with spherical alumina, these changes had a negligible effect. In the case of the mixture with irregular alumina, following a slight enlargement of the metal particles (from 26 to 30 μm) and a slight reduction of the size of ceramic particles (from 22 to 20 μm), a small shift of the maximum value of DE_{mix} towards lower ceramic contents of the mixture and a slight reduction of the ceramic content of the sprayed coating were observed. In the opposite situation (d_p= 20 and d_{cer}= 30 μm), a shift of the maximum value of DE_{mix} towards higher ceramic contents of the mixture and an obvious increase in the ceramic content of the coating were identified. In this case, the deposition efficiency of the mixture was found to slightly decrease in value in the region with c_V< 0.4, but it was increasing in the region with c_V> 0.4. From Fig. 7(b), it can be concluded that, for spraying coatings with a high ceramic content (in the region of c_V= 0.4–0.8), one has to choose ceramic powders with a larger size of ceramic particles in comparison with the average size of metal particles.

In practice, when spraying mixtures of metals with ceramics, one can pursue two different goals. In the first case, a ceramic is added to a metal powder in order to increase the deposition efficiency of the mixture, with the ceramic content of the sprayed coating having been made as small as possible. Here, it is desired that the deposition efficiency would reach its maximum value at the possibly lowest ceramic content of the mixture. Thus, in order to solve such problems, one has to use a ceramic powder with a mean particle size smaller than the mean particle size of the metal powder. In the second case, it is required to obtain a coating with a maximum ceramic content. This raises a dilemma. On the one hand, on increasing the ceramic content of the mixture, the ceramic content of the

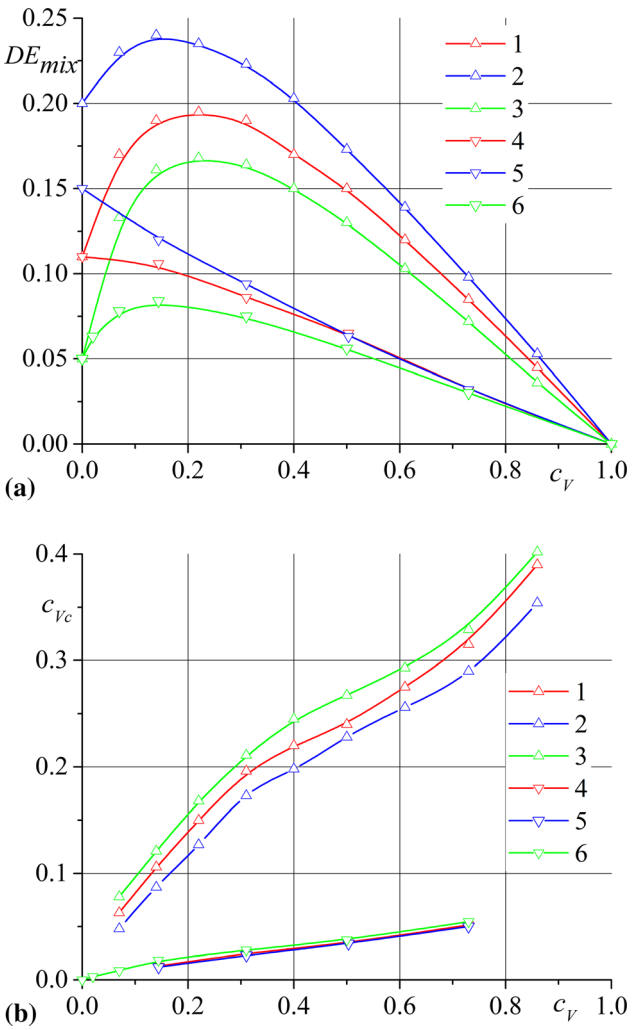

Fig. 8 The simulated deposition efficiency of the mixture (a) and the ceramic content of the sprayed coating (b). Irregular alumina: 1—initial value, p= 0.11; 2—increased value, p= 0.2; 3—lower value, p= 0.05; spherical alumina: 4—initial value, p= 0.11; 5—increased value, p= 0.15; 6—lower value, p= 0.05.

sprayed coating also increases, but, simultaneously, the deposition efficiency of the mixture decreases. In any case, the simulation results show that, at a volumetric ceramic content in powder more than 0.4, it can be seen that it is more advantageous to use a ceramic powder for this purpose with a mean particle size larger than that of the metal powder.

Effect Due to the Deposition Efficiency of Metal Powder

Since the properties of a powder strongly depend on the conditions of its preparation and storage (or on the conditions of a pre-treatment procedure such as drying, annealing, quenching, etc.), we can hypothesize that the deposition efficiency of pure metal powder p may be a varied parameter. Below, we analyze a situation in which the pure metal powder adheres to the coating surface with a deposition efficiency larger than 0.11, say, 0.2, and, alternatively, with a deposition efficiency lower than 0.11, say, 0.05. The calculation results pertaining to those cases are shown in Fig. 8.

In the case of the mixture with irregular alumina, it can be seen that, on increasing the deposition efficiency of pure metal powder, the deposition efficiency of the mixture increases while the maximum shifts toward the lower ceramic contents of the mixture (Fig. 8a, curve 2). In this case, the ceramic content of the sprayed coating reduces slightly (Fig. 8b, curve 2). In the opposite case, a decrease in the deposition efficiency of the mixture is observed, although the maximum stays occupying approximately the same position (Fig. 8a, curve 3). In the latter case, the ceramic content of the coating increases slightly (Fig. 8b, curve 3). It is noteworthy that a fairly large change in the probability of adherence of pure metal powder p leads to distinctly observed yet not very large deviations in the deposition efficiency of the mixture and in the ceramic contents of the coating.

In the case of the mixture with spherical alumina, as can be seen from Fig. 8(b), the alumina content in coating is not essentially changed. However, one can see in Fig 8(a) that, when decreasing the deposition efficiency of pure metal powder, the behavior of the mixture deposition efficiency changes from a monotonic drop into a non-monotonic with the maximum. Noticeable changes are only in the range where the volumetric content of alumina in powder is lower than 0.2.

Before the conclusion, some remarks are necessary. In the present paper, particle shape was suggested to be spherical. Developed computer software allows the calculating of only simple circle shapes, because it is not an easy task to construct a computer code to represent/generate random irregular shapes. We hope to do this in the future. On the one hand, it is a limitation of the model, while on the other hand, it is an advantage due to its simplicity. In the present paper, it is shown that limiting the shape of the particles just to circles, but adjusting only three main input parameters p, p_a , and p_{cer}, it is possible to reproduce experimental data (Ref 21,22) on the dependence of the output parameters (i.e., deposition efficiency and ceramic content in the coating) on the ceramic content in powder mixtures for irregular shapes of particles. We suggest that the input parameters depend upon the shape of the particles. Hence, we suggest that the output parameters are dependent from the particle shapes mainly via these three input parameters. From this point of view, it is not important what cold spray conditions (for example, low-pressure or high-pressure) are considered, as these three input parameters determine the behavior of the output parameters. Thus, we divide the problem of the deposition of metal and ceramic mixtures into two independent parts: the present paper dedicated to the part mentioned above, while the second part (which is in progress) should be dedicated to how these three input parameters can be estimated taking into account the cold spray conditions. It should be noted that at present this is a challenging task because they are dependent upon many parameters (particle velocities, temperatures, shapes, materials, etc.).

In the present paper, the model is validated only for conditions of low deposition efficiencies, i.e., using data presented in (Ref 21,22). Of course, it would be desirable to validate it for other cold spray conditions; for example, for high-pressure conditions when the deposition efficiency of the metal is higher than those tested in the present paper. It concerns first of all ceramic contents in coatings, but it is difficult to find reliable experimental data in the literature. As for deposition efficiency, some verification is presented in (Ref 13), where it was shown that when the deposition efficiency of metal is high enough then an admixture of ceramic powders leads to monotonic lowering of the mixture deposition efficiency with an increase in the ceramic content in powder mixtures. In general, the more diversified validation will be the topic of future work.

Conclusion

A numerical model, based on Monte Carlo calculations, has been reported for the first time to take into account both the effect due to the adherence of ceramic particles to the coating surface and the effect due to the discontinuity of both the activated surface area and the surface area occupied by ceramic particles. The calculation results were compared with the available experimental data. It is shown that, with a proper choice of the values of the involved model parameters, one can invent an adequate quantitative

description both of the behavior of the deposition efficiency of the mixture and of the behavior of the ceramic content of the coating.

Acknowledgment The reported study was funded by RFBR and ROSATOM, project number 20-21-00046 using equipment of the Joint-Use Center "Mechanics" of ITAM SB RAS.

References

1. A.P. Alkhimov, V.F. Kosarev and A.N. Papyrin, Method of Cold Gas-Dynamic Spraying, *Dokl. Akad. Nauk SSSR*, 1990, **315**, p 1062-1065.
2. A. Papyrin, V. Kosarev, S. Klinkov, A. Alkhimov and V. Fomin, *Cold Spray Technology*, Elsevier, Amsterdam, 2007.
3. Kashirin, A.I., Klyuev, O.F., Buzdygar, T.V. Apparatus for gas-dynamic coating, US Patent 6,402,050, 2002
4. V.F. Kosarev, S.V. Klinkov, A.A. Sova and I. Smurov, Deposition of Multi-component Coatings by Cold Spray, *Surf. Coat. Technol.*, 2008, **202**, p 5858-5862.
5. A. Shkodkin, A. Kashirin, O. Klyuev and T. Buzdygar, Metal Particle Deposition Stimulation by Surface Abrasive Treatment in Gas Dynamic Spraying, *J. Therm. Spray Technol.*, 2006, **15**(3), p 382-386.
6. E. Irissou, J.-G. Legoux, B. Arsenault and Ch. Moreaus, Investigation of Al-Al_2O_3 Cold Spray Coating Formation and Properties, *J. Therm. Spray Technol.*, 2007, **16**(5-6), p 661-668.
7. A. Sova, A. Papyrin and I. Smurov, Influence of Ceramic Powder Size on Process of Cermet Coating Formation by Cold Spray, *J. Therm. Spray Technol.*, 2009, **18**(4), p 633-641.
8. K. Spencer, D.M. Fabijanic and M.-X. Zhang, The Use of Al-Al_2O_3 Cold Spray Coatings to Improve the Surface Properties of Magnesium Alloys, *Surf. Coat. Technol.*, 2009, **204**, p 336-344.
9. Q. Wang, K. Spencer, N. Birbilis and M.-X. Zhang, The Influence of Ceramic Particles on Bond Strength of Cold Spray Composite Coatings on AZ91 Alloy Substrate, *Surf. Coat. Technol.*, 2010, **205**, p 50-56.
10. M. Yandouzi, A.J. Böttger, R.W.A. Hendrikx, M. Brochu, P. Richer, A. Charest and B. Jodoin, Microstructure and Mechanical Properties of B_4C Reinforced Al-Based Matrix Composite Coatings Deposited by CGDS and PGDS Processes, *Surf. Coat. Technol.*, 2010, **205**, p 2234-2246.
11. A. Sova, D. Pervushin and I. Smurov, Development of Multimaterial Coatings by Cold Spray and Gas Detonation Spraying, *Surf. Coat. Technol.*, 2010, **205**, p 1108-1114.
12. K. Spencer, D.M. Fabijanic and M.-X. Zhang, The Influence of Al_2O_3 Reinforcement on the Properties of Stainless Steel Cold Spray Coatings, *Surf. Coat. Technol.*, 2012, **206**, p 3275-3282.
13. S.V. Klinkov and V.F. Kosarev, Cold Spraying Activation Using an Abrasive Admixture, *J. Therm. Spray Technol.*, 2012, **20**(4), p 837-844.
14. H. Bu, M. Yandouzi, Ch. Lu, D. MacDonald and B. Jodoin, Cold Spray Blended Al+$Mg_{17}Al_{12}$ Coating for Corrosion Protection of AZ91D Magnesium Alloy, *Surf. Coat. Technol.*, 2012, **207**, p 155-162.
15. X.K. Suo, Q.L. Suo, W.Y. Li, M.P. Planche and H.L. Liao, Effects of SiC Volume Fraction and Particle Size on the Deposition Behavior and Mechanical Properties of Cold-Sprayed AZ91D/SiC Composite Coatings, *J. Therm. Spray Technol.*, 2014, **23**(1-2), p 91-97.
16. J.M. Shockley, S. Descartes, P. Vo, E. Irissou and R.R. Chromik, The Influence of Al_2O_3 Particle Morphology on the Coating Formation and Dry Sliding Wear Behavior of Cold Sprayed Al-Al_2O_3 Composites, *Surf. Coat. Technol.*, 2015, **270**, p 324-333.
17. O. Tazegul, V. Dylmishi and H. Cimenoglu, Copper Matrix Composite Coatings Produced by Cold Spraying Process for Electrical Applications, *Arch. Civ. Mech. Eng.*, 2016, **16**, p 344-350.
18. V.F. Kosarev, A.A. Polukhin, N.S. Ryashin, V.M. Fomin and V.S. Shikalov, Influence of the Powder Mixture Composition on the Deposition Coefficient and the Properties of Ni+B_4C CGDS Coatings, *Mech. Solids*, 2017, **52**(4), p 457-464.
19. V.M. Fomin, A.A. Golyshev, V.F. Kosarev, A.G. Malikov, A.M. Orishich, N.S. Ryashin, A.A. Filippov and V.S. Shikalov, Creation of Heterogeneous Materials on the Basic of B_4C and Ni Powders by the Method of Cold Spraying with Subsequent Layer-by-Layer Laser Treatment, *J. Appl. Mech. Tech. Phys.*, 2017, **58**(5), p 947-955.
20. X. Bai, J. Tang, J. Gong and X. Lu, Corrosion Performance of Al-Al_2O_3 Cold Sprayed Coatings on Mild Carbon Steel Pipe Under Thermal Insulation, *Chin. J. Chem. Eng.*, 2017, **25**, p 533-539.
21. R. Fernandez and B. Jodoin, Cold Spray Aluminum-Alumina Cermet Coatings: Effect of Alumina Content, *J. Therm. Spray Technol.*, 2018, **27**, p 603-623.
22. R. Fernandez and B. Jodoin, Cold Spray Aluminum-Alumina Cermet Coatings: Effect of Alumina Morphology, *J. Therm. Spray Technol.*, 2019, **28**, p 737-755.
23. N.H. Tariq, L. Gyansah, X. Qiu, H. Du, J.Q. Wang, B. Feng, D.S. Yan and T.Y. Xiong, Thermo-Mechanical Post-Treatment: A Strategic Approach to Improve Microstructure and Mechanical Properties of Cold Spray Additively Manufactured Composites, *Mater. Des.*, 2018, **156**, p 287-299.
24. N.H. Tariq, L. Gyansah, J.Q. Wang, X. Qiu, B. Feng, M.T. Siddique and T.Y. Xiong, Cold Spray Additive Manufacturing: A Viable Strategy to Fabricate Thick B_4C/Al Composite Coatings for Neutron Shielding Applications, *Surf. Coat. Technol.*, 2018, **339**, p 224-236.
25. N.H. Tariq, L. Gyansah, X. Qiu, C. Jia, H.B. Awais, C.Z.H. Du, J. Wang and T. Xiong, Achieving Strength-Ductility Synergy in Cold Spray Additively Manufactured Al/B_4C Composites Through a Hybrid Post-Deposition Treatment, *J. Mater. Sci. Technol.*, 2019, **35**, p 1053-1063.
26. G. Huang, Fu. Wei, Li. Ma, X. Li and H. Wang, Cold Spraying B_4C Particles Reinforced Aluminum Coatings, *Surf. Eng.*, 2019, **35**(9), p 772-783.
27. S.A. Alidokht, S. Yue and R.R. Chromik, Effect of WC Morphology on Dry Sliding Wear Behavior of Cold-Sprayed Ni-WC Composite Coatings, *Surf. Coat. Technol.*, 2019, **357**, p 849-863.
28. L. Zhang, S. Yang, X. Lu and X. Jie, Wear and Corrosion Resistance of Cold-Sprayed Cu-Based Composite Coatings on Magnesium Substrate, *J. Therm. Spray Technol.*, 2019, **28**, p 1212-1224.
29. W. Chen, Y. Yu, J. Ma, S. Zhu and We. Liu, J. Yang, , Low-Pressure Cold Spraying of Copper-Graphite Solid Lubricating Coatings on Aluminum Alloy 7075-T651, *J. Therm. Spray Technol.*, 2019, **28**, p 1688-1698.
30. L. Wang, F. Wang, S. Li and Y. Wang, Microstructure and Application of Alumina-Supported Cu-Based Coating Prepared by Cold Spray, *Surf. Coat. Technol.*, 2019, **362**, p 113-123.
31. Z. Zhang, F. Liu, E.-H. Han, Xu. Long and P.C. Uzoma, Effects of Al_2O_3 on the Microstructures and Corrosion Behavior of Low-Pressure Cold Gas Sprayed Al 2024-Al_2O_3 Composite Coatings on AA 2024-T3 Substrate, *Surf. Coat. Technol.*, 2019, **370**, p 53-68.
32. Z. Khalkhali, K.S. Rajan and J.P. Rothstein, Peening Effect of Glass Beads in the Cold Spray Deposition of Polymeric Powders, *J. Therm. Spray Technol.*, 2020, **29**, p 657-669.

33. J.-M. Lamarre and F. Bernier, Permanent Magnets Produced by Cold Spray Additive Manufacturing for Electric Engines, *J. Therm. Spray Technol.*, 2019, **28**, p p1709-1717.
34. I. Finnie, Erosion of Surfaces by Solid Particles, *Wear*, 1960, **3**(2), p 87-103.
35. J.H. Neilson and A. Gilchrist, Erosion by a Stream of Solid Particles, *Wear*, 1968, **11**(2), p 111-122.